Intravital imaging of metastatic behavior through a mammary imaging window

Dmitriy Kedrin[1,4], Bojana Gligorijevic[1,2,4], Jeffrey Wyckoff[1,2], Vladislav V Verkhusha[1,2], John Condeelis[1,2], Jeffrey E Segall[1] & Jacco van Rheenen[1–3]

We report a technique to evaluate the same tumor microenvironment over multiple intravital imaging sessions in living mice. We optically marked individual tumor cells expressing photoswitchable proteins in an orthotopic mammary carcinoma and followed them for extended periods through a mammary imaging window. We found that two distinct microenvironments in the same orthotopic mammary tumor affected differently the invasion and intravasation of tumor cells.

The early steps of metastasis are characterized by tumor cells invading the stroma (invasion) and entering the blood (intravasation)[1,2]. Short-term tracking of individual cells inside fluorescent tumors by intravital imaging has revealed dramatic heterogeneity in tumor cell invasion and intravasation[3]. However, long-term tracking of individual cells is required to quantify these behaviors and to determine the fates of cells in specific tumor microenvironments. Imaging techniques that rely on surgical dissection to expose the imaging site have limitations for long-term experiments such as (i) tissue dehydration and impaired thermoregulatory control and/or animal survival upon surgical dissection, (ii) possible effects of prolonged anesthesia exposure, and (iii) a limited field of view. These limitations can be overcome by studying tumors through a dorsal skinfold chamber[4]. The use of dorsal skinfold chambers, however, limits the experiments to tumor models based on cell lines and, for many tumors, a non-orthotopic environment. For example, invasion and intravasation of breast tumor cells is highly dependent on the specific local microenvironment[5], which may not exist in the nonmammary environments such as the dorsal skinfold chamber site[4]. Here we describe the integration of a mammary imaging window (MIW) with photoswitchable fluorescent protein labeling. This technique enabled tracking of selected tumor cell subpopulations in different breast tumor microenvironments and monitoring of cell migration for more than 24 h.

To image orthotopic (in the natural, mammary gland environment) breast tumors intravitally at high resolution for prolonged times, we developed a MIW that can be placed on top of the mammary gland of a mouse (**Fig. 1a**). The protocol for these animal studies was approved by the Institutional Animal Care and Use Committee for the Albert Einstein College of Medicine. The MIW contains two plastic rings that form a mount for a glass coverslip (**Fig. 1a**). The mount has holes that facilitate suturing into the skin, and the glass coverslip assures the optimal working distance and refraction index for high-resolution imaging (for details on equipment used for imaging, see **Supplementary Fig. 1** online). Whereas surgical dissection of the skin overlaying the imaging site allows for several hours of data collection and is usually a terminal procedure, imaging through the MIW extended the imaging time to multiple days (up to 21 d). Implantation of the MIW did not alter inflammation or the microenvironment (measured 24 h after implantation), or tumor growth over 9 d (**Supplementary Fig. 2** online). However, expression of the photoswitchable protein we used, Dendra2, may alter blood-vessel density (**Supplementary Fig. 2c**).

To locate the same subpopulation of cells for cell tracking in each of the imaging sessions, reference points were required[6]. In the fast-changing tissue topology of the tumor, the use of fixed reference points is limited, and therefore we used photoswitchable fluorescent proteins[7,8] as photomarkers of the cells of interest. These proteins are a new group of GFP-like fluorophores that allow labeling and tracking of a single cell or a group of cells[9–12]. We stably expressed the photoswitchable protein Dendra2 in the metastatic breast cancer line MTLn3. Dendra2 resembles GFP in its spectrum before photoswitching, but exposure to blue light (for example, 405 nm) can induce an irreversible red shift >150 nm in the excitation and emission spectra of the chromophore[13]. After the photoswitch, the red fluorescence stably increases up to 250-fold both *in vitro* (**Fig. 1b**) and *in vivo* (**Fig. 1c**), resulting in red/green contrast of up to 850 and allowing us to track cells marked this way. Five days after photoswitching, the red fluorescence of the photoswitched cells was still 31-fold higher than the red fluorescence of nonswitched cells, which enabled us to recognize the highlighted cells *in vivo* for extended amounts of time after the photoswitch (**Fig. 1d**).

We photoswitched regions of the Dendra2-MTLn3 tumor containing one to hundreds of cells and imaged them through the MIW (**Fig. 1e**, **Supplementary Movies 1** and **2**, and **Supplementary**

[1]Department of Anatomy and Structural Biology, [2]Gruss Lipper Biophotonics Center, Albert Einstein College of Medicine of Yeshiva University, 1300 Morris Park Avenue, Bronx, New York 10461, USA. [3]Hubrecht Institute, Royal Netherlands Academy of Arts and Sciences and University Medical Center Utrecht, Uppsalalaan 8, 3584CT Utrecht, The Netherlands. [4]These authors contributed equally to this work. Correspondence should be addressed to J.v.R. (j.vanrheenen@niob.knaw.nl), J.C. (condeeli@aecom.yu.edu) or J.E.S. (segall@aecom.yu.edu).

RECEIVED 25 AUGUST; ACCEPTED 10 OCTOBER; PUBLISHED ONLINE 9 NOVEMBER 2008; DOI:10.1038/NMETH.1269

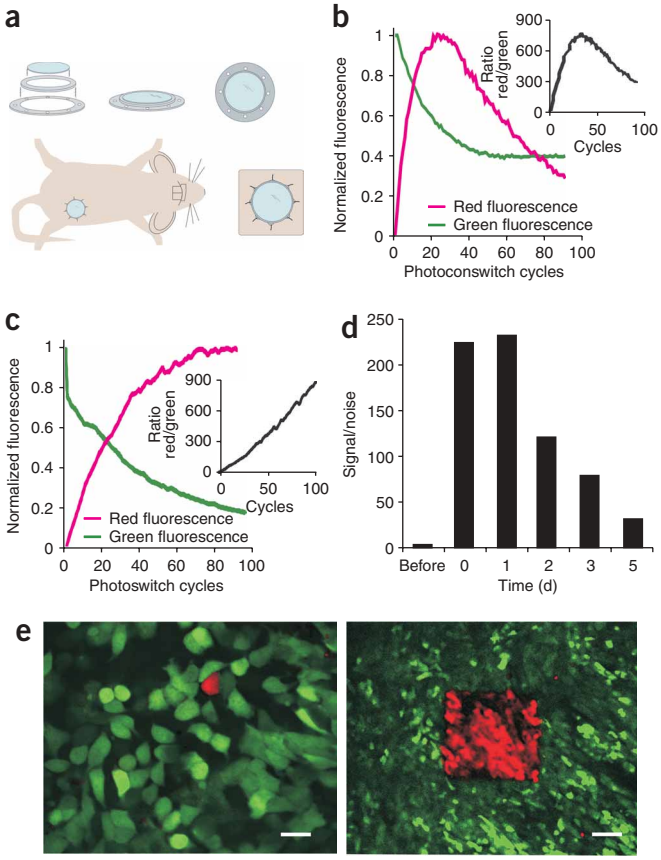

Figure 1 | The MIW allows for long-term, high-resolution imaging of the orthotopic tumors. (**a**) To assemble the MIW, a coverslip was mounted on a plastic frame consisting of two plastic rings (top) and was surgically implanted on top of the mammary gland or mammary tumor of a mouse (bottom). (**b**,**c**) Average changes in fluorescence for Dendra2, as measured in a region of interest, in cells *in vitro* (**b**) or *in vivo* after injection of the Dendra2-expressing MTLn3 tumor cells into the abdominal mammary fat pad (**c**) upon photoswitching. The values were normalized to the highest fluorescence level in the red fluorescence channel and the initial fluorescence level in the green fluorescence channel. Insets, ratio of the non-normalized red/green fluorescence. (**d**) Cells in Dendra2-tumors were photoswitched through the MIW and the red fluorescence was quantified before photoswitching (before), immediately after photoswitching (0 d) and at indicated times thereafter. The values were normalized to the red fluorescence level before photoswitching. (**e**) Photoswitching of Dendra2-expressing MTLn3 tumor cells *in vivo* in regions of interest ranging from one cell (left; scale bar, 10 μm) to hundreds of cells (right; scale bar, 75 μm) through the MIW. Shown are combined images from the green and red fluorescence channels using an 'or' function. Only the pixels in the red channel that are above background are shown, and for all other pixels, the green channel is shown.

Fig. 3 online). As cells in the tumor migrated and invaded, the distribution of these cells relative to blood vessels and other tumor cells changed over time. By selectively photoswitching the fluorophore in a group of cells (**Fig. 1e**), we visualized changes in distribution of cells in the tumor microenvironment. Twenty four hours after photo-switching, we recorded images of the non-photoswitched tumor cells (Dendra2 green fluorescence), photoswitched cells (Dendra2 red fluorescence), extracellular matrix (collagen was visualized by reflectance in **Fig. 2a** or second-harmonic-generation imaging in **Supplementary Movie 3** online) and blood vessels (fluorescent dextrans were used for vessel labeling; **Supplementary Movie 4** online). Notably, some photoswitched regions showed dramatic migration and invasion of the surrounding microenvironment (**Fig. 2a**).

The tumor perivascular microenvironment (tumor tissue surrounding blood vessels) was enriched in tumor-associated macrophages and extracellular matrix. This microenvironment supports metastatic behavior, including inhibition of proliferation and stimulation of migration, invasion and intravasation[5,14]. This suggests the existence of distinct mammary tumor

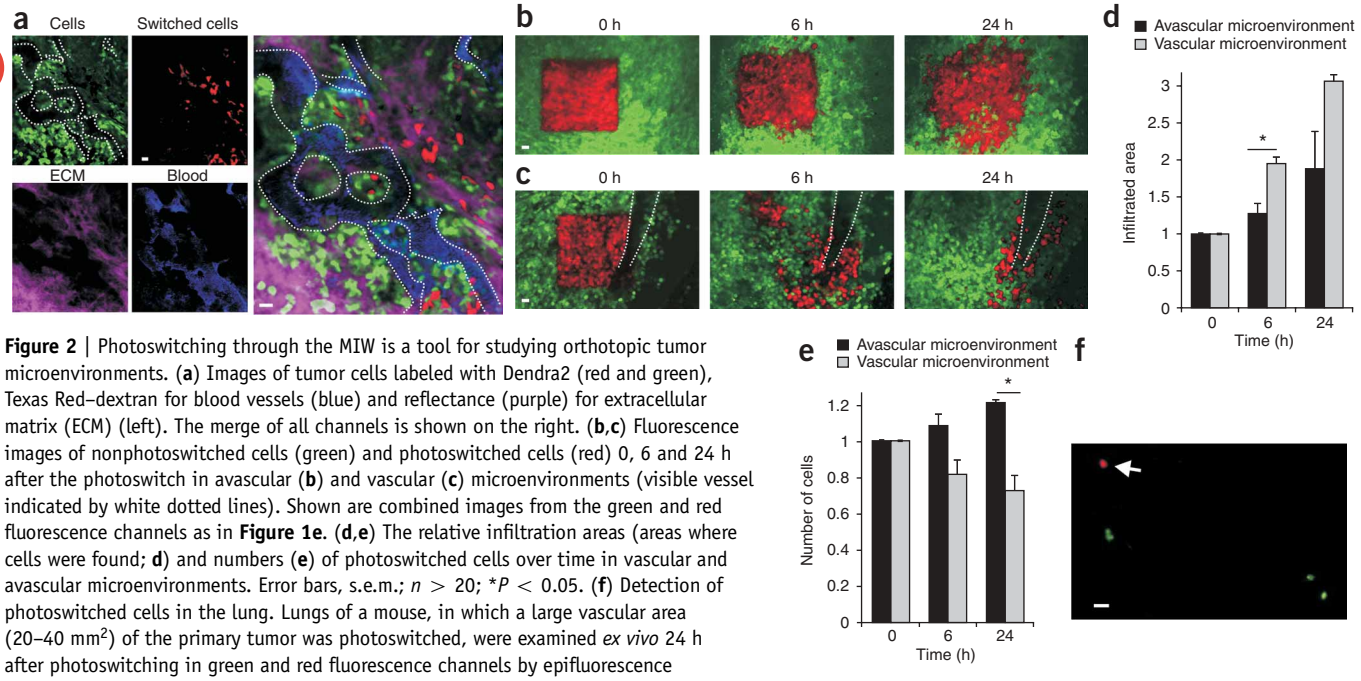

Figure 2 | Photoswitching through the MIW is a tool for studying orthotopic tumor microenvironments. (**a**) Images of tumor cells labeled with Dendra2 (red and green), Texas Red–dextran for blood vessels (blue) and reflectance (purple) for extracellular matrix (ECM) (left). The merge of all channels is shown on the right. (**b**,**c**) Fluorescence images of nonphotoswitched cells (green) and photoswitched cells (red) 0, 6 and 24 h after the photoswitch in avascular (**b**) and vascular (**c**) microenvironments (visible vessel indicated by white dotted lines). Shown are combined images from the green and red fluorescence channels as in **Figure 1e**. (**d**,**e**) The relative infiltration areas (areas where cells were found; **d**) and numbers (**e**) of photoswitched cells over time in vascular and avascular microenvironments. Error bars, s.e.m.; $n > 20$; $^*P < 0.05$. (**f**) Detection of photoswitched cells in the lung. Lungs of a mouse, in which a large vascular area (20–40 mm^2) of the primary tumor was photoswitched, were examined *ex vivo* 24 h after photoswitching in green and red fluorescence channels by epifluorescence microscopy. Arrow, red tumor cell photoswitched in and disseminated from the primary tumor. We determined 0.009 ± 0.007 (s.e.m.) red cells and 1.4 ± 0.33 green-fluorescent cells per mm^2 lung, resulting in a green/red ratio of 152 ± 0.81. Scale bars, 30 μm (**a**–**c**) and 20 μm (**f**).

microenvironments within the same tumor with different rates of invasion and intravasation. However, the long-term implications of these observations required the ability to image distinct microenvironments inside the same mammary gland over a 24-h period. To quantify invasion and intravasation within distinct mammary gland microenvironments, we photoswitched square regions (~300 cells) in different tumor microenvironments of the same orthotopically grown tumor (**Supplementary Fig. 3**), focusing on regions lacking and containing detectable blood vessels (**Fig. 2b**,**c**). We located the photoswitched red cells by acquiring *z*-dimension stacks of red and green fluorescence images of the same regions at 0, 6 and 24 h after photoswitching. In regions not containing detectable vessels there was limited migration, and the number of photoswitched cells increased (**Fig. 2b**,**d**,**e**), suggesting that this microenvironment does not support metastatic behavior. In contrast, photoswitched cells in the vascular microenvironment infiltrated larger areas (**Fig. 2c**,**d**) and even migrated to sites outside of the field of view. Moreover, photoswitched cells in this vascular microenvironment lined up along the blood vessel (**Fig. 2c**), with a concomitant decrease in the number of red-fluorescent tumor ells and the appearance of red-fluorescent tumor cells in the lung (**Fig. 2c**,**e**,**f** and **Supplementary Methods** online). From these experiments we concluded that cell behavior is determined by the surrounding microenvironment, and that the vascular microenvironment promotes invasion and intravasation of tumor cells.

Although the existence of different tumor microenvironments has been reported previously[5], the quantitative analysis of such microenvironments in the same tumor with spatial and temporal resolution is not possible with previous techniques. The combination of photoswitchable proteins with the MIW allowed for such analysis, as a distinct group of cells can be photomarked in any location in the primary tumor and tracked over time without long-term anesthesia. Furthermore, the high stability of Dendra2 allowed us to freeze-fix the tissues and analyze them by microscopy without additional labeling. A limitation of Dendra2 is that a limited number of excitation wavelengths can be used. For example, as violet light causes a switch, 4,6-diamidino-2-phenylindole (DAPI) stains should only be used after imaging other wavelengths as DAPI imaging would cause all green-fluorescent cells to then become red-fluorescent. Nevertheless, through the MIW the formation of tumors from injection of cells in the mammary gland can be followed for days, which is not possible in surgically dissected areas. This also opens the possibility to study fluorescently tagged proteins that have lethal effects if stably expressed but can be studied in transiently transfected cells. For example, transiently transfected cells expressing membrane-targeted GFP and injected into the mammary gland can be imaged with high resolution through the MIW (**Supplementary Fig. 4a** online). Although this would also be possible with the dorsal skinfold chamber[4], imaging through the MIW allows studies of cell behavior in their physiological breast microenvironments and moreover, the MIW technology can be extended to tumors of transgenic origin, such as the MMTV-PyMT tumor model (**Supplementary Fig. 4b**). Such tumor models allow the investigation of different stages of tumor progression[15] in contrast to cell line–derived xenografts. The combined use of MIW and photomarking cells to revisit chosen subpopulations of cells is an important capability not only in tumor studies but any studies related to cell motility and morphogenesis. Visualization of infectious agents and immune responses, or the progression of chronic inflammation, are other examples of the potential applications of the technique described here.

Note: Supplementary information is available on the Nature Methods website.

ACKNOWLEDGMENTS

This work was supported by US Department of Defense (BC061403 to D.K.), US National Institutes of Health (U54GM064346 to J.v.R.; CA100324 to J.C., J.E.S. and J.W.; U54CA126511 to J.C. and B.G.; and GM070358 and GM073913 to V.V.V.). We thank the staff of the Analytical Imaging Facility and D. Entenberg for help with microscopy, the immunohistochemistry facility for help with histology, M. Rottenkolber for help in fabrication of the imaging box, J. Pollard (Albert Einstein College of Medicine) for providing the F4/80 antibody, S. Garofalo for technical assistance, and members of the Condeelis, Segall, Cox and Verkhusha laboratories for discussions.

Published online at http://www.nature.com/naturemethods/
Reprints and permissions information is available online at http://npg.nature.com/reprintsandpermissions/

1. Condeelis, J. & Segall, J.E. *Nat. Rev. Cancer* **3**, 921–930 (2003).
2. Gupta, G.P. & Massague, J. *Cell* **127**, 679–695 (2006).
3. Sidani, M. *et al. J. Mammary Gland Biol. Neoplasia* **11**, 151–163 (2006).
4. Lehr, H.A. *et al. Am. J. Pathol.* **143**, 1055–1062 (1993).
5. Wyckoff, J.B. *et al. Cancer Res.* **67**, 2649–2656 (2007).
6. Bins, A.D. *et al. BMC Biotechnol.* **7**, 2 (2007).
7. Gurskaya, N.G. *et al. Nat. Biotechnol.* **24**, 461–465 (2006).
8. Lukyanov, K.A., Chudakov, D.M., Lukyanov, S. & Verkhusha, V.V. *Nat. Rev. Mol. Cell Biol.* **6**, 885–891 (2005).
9. Gray, N.W., Weimer, R.M., Bureau, I. & Svoboda, K. *PLoS Biol.* **4**, e370 (2006).
10. Sato, T., Takahoko, M. & Okamoto, H. *Genesis* **44**, 136–142 (2006).
11. Hatta, K., Tsujii, H. & Omura, T. *Nat. Protoc.* **1**, 960–967 (2006).
12. Post, J.N., Lidke, K.A., Rieger, B. & Arndt-Jovin, D.J. *FEBS Lett.* **579**, 325–330 (2005).
13. Chudakov, D.M., Lukyanov, S. & Lukyanov, K.A. *Nat. Protocols* **2**, 2024–2032 (2007).
14. Condeelis, J. & Pollard, J.W. *Cell* **124**, 263–266 (2006).
15. Lin, E.Y. *et al. Am. J. Pathol.* **163**, 2113–2126 (2003).